Supplemental information

Stabilizing the commensurate charge-density wave (CCDW) 1T-Tantalum Disulfide at higher temperatures via Potassium Intercalation

Rui Zhao[1,2], Benjamin Grisafe[3], Ram Krishna Ghosh[3,4], Ke Wang[5], Suman Datta[3], Joshua Robinson[1,2*]

[1] Department of Materials Science and Engineering, The Pennsylvania State University, University Park, PA, 16802, USA
[2] The Center for 2-Dimensional and Layered Materials, The Pennsylvania State University, University Park, PA, 16802, USA
[3] Department of Electrical Engineering, University of Notre Dame, Notre Dame, IN, 46556, USA
[4] Special Centre for Nanoscience, Jawaharlal Nehru University, New Delhi 110067, India
[5] Materials Research Institute, The Pennsylvania State University, University Park, PA, 16802, USA
Corresponding author: * email: jrobinson@psu.edu

Experiment details of KCl enhanced deposition of TaS2

Growth set-up is schematically shown in Fig. 1a. KCl enhanced growth was carried out in a 2" tube furnace, which has two temperature control zones (T_1 and T_2). The largest temperature difference between two zones is set to be 300ºC. TaS_2 precursor was acquired based on the method introduced in our previous report[1]. TaS_2 precursor and KCl are mixed at certain weight ratios and put in the center of an alumina crucible, which is situated at the center of the furnace heating zones (between T_1 and T_2 zones). The second alumina crucible is put in the center of T_2 zone, whose temperature profile is shown in Fig. S1. Deposition substrates (sapphire, SiO_2/Si, or epitaxial graphene) are put on top of the second crucible and face-up growth is expected. The carrier gas is high purity argon gas. The flow rate is set to be 100sccm and flow direction is from T_1 to T_2. The entire synthesis process is carried out at a fixed pressure level (710torr).

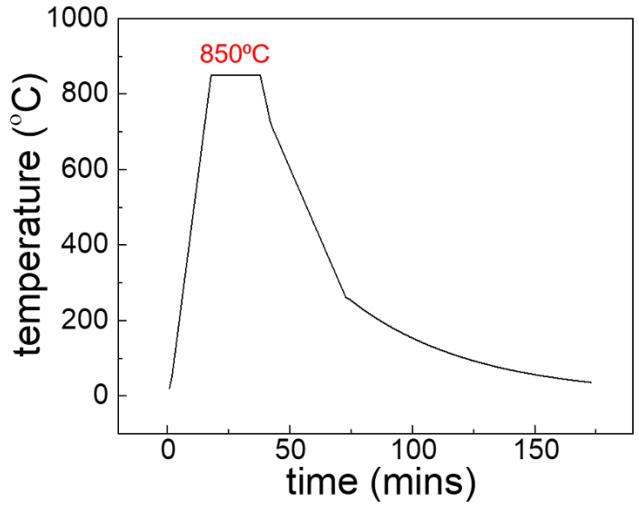

Figure S1 Temperature profile of T_2 zone for material deposition and growth

Cross section TEM and EDS of intercalated 1T-TaS2 before electric drive

Cross section TEM was conducted on the K^+ intercalated 1T-TaS_2 before electric field was applied. Fig. S2a is the EDX mapping of K ion through the intercalated samples. Based on the image, layer structure is maintained after K^+ ion is incorporated. K^+ ion is uniformly distributed through the 1T-TaS_2 flake. Fig. S2b records EDX peak signal collected from the sample. Weak K^+ ion signal indicates very low intercalation level in this flake under study. This may also explain why the layer structure is more intact than the one shown in Fig. 2f. Structural change in 1T-TaS_2 would be promoted once the intercalated K^+ reaches a certain level as reflected in Fig. 1c.

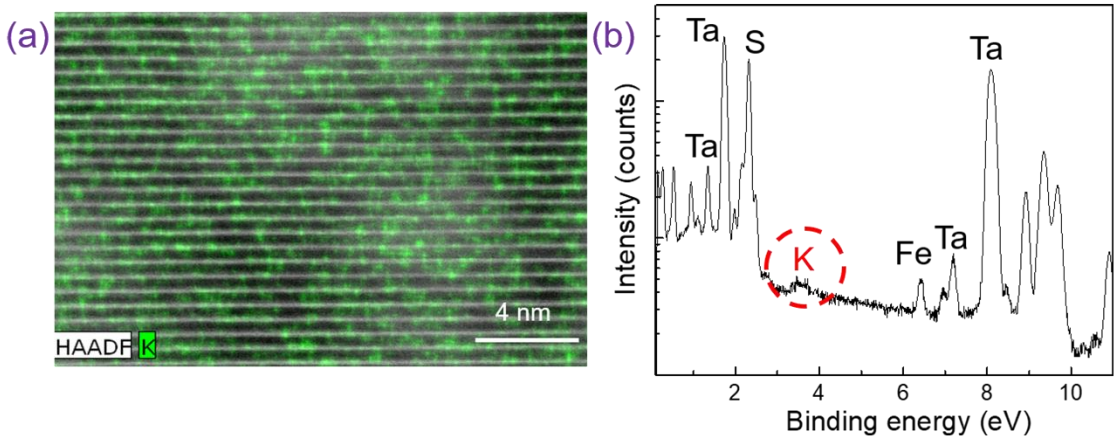

Figure S2 (a) EDX mapping of K^+ ion in the intercalated 1T-TaS_2. (b) EDX element profile corresponding to the image in (a). As indicated, K^+ ion intercalation level is low in this flake, whose layer structure is more intact than the one depicted in Fig. 2f

Sheet resistance of pure 1T-TaS_2 and intercalated 1T-TaS_2 via CVD process

Sheet resistance of pure CVD 1T-TaS_2 flake and intercalated CVD 1T-TaS_2 flake are included in Fig. S3. Comparing with exfoliated 1T-TaS_2 of similar thicknesses[2,3], both abovementioned flakes demonstrate higher sheet resistance. This is largely due to the higher level of defects, which is well-studied for CVD flakes[4–6]. Besides, intercalated CVD flake even shows slightly larger resistance, which is probably due to the lattice distortion and higher defects levels brought about by K^+ ion intercalation.

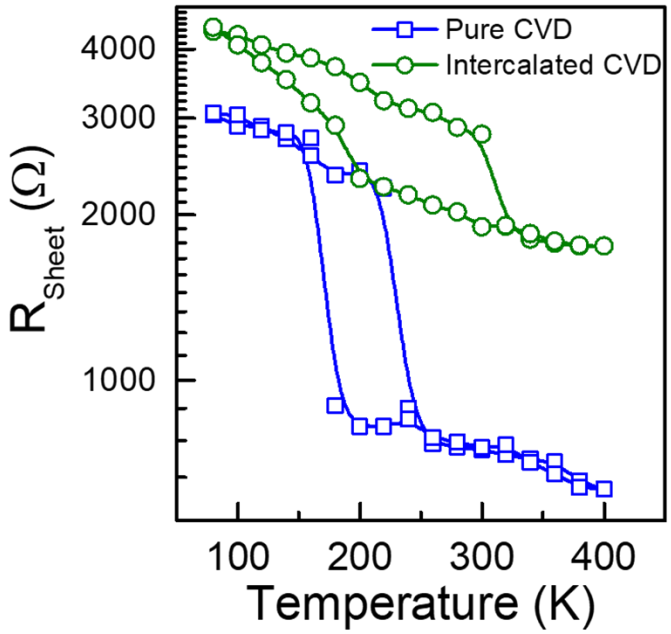

Figure S3 Sheet resistance of pure CVD and intercalated CVD 1T-TaS_2 flake

DFT method

To evaluate the structural and electronic properties of K intercalated 1T-TaS2, we have used Density Functional Theory (DFT) within the generalized gradient approximations (GGA) as implemented in the QuantumWise, Atomistix Toolkit (ATK)[7]. In our calculations, the valence band wave functions of different atoms have been explicitly treated as a linear combination of atomic orbitals (LCAO). We have considered Perdew-Burke-Ernzerhof (PBE) approximation for the exchange-correlation functional along with norm-conserving SG15 pseudopotentials (a set of Optimized Norm-Conserving Vanderbilt (ONCV) pseudopotentials)[8,9] which are very close to well-converged plane wave basis sets. We have also included the Grimme's DFT-D2 functional to treat the long-range van der Waals interactions of the layers. In order to produce the effect of K intercalation or K substitution in 1T-TaS2, we have used a 2×2×2 supercell of 1T-TaS2 and for that we have used a 4×4×4 Monkhorst–Pack k-point mesh centered at Γ and a and mesh cut-off energy of 150 Ry on a real space grid of charge density and potentials that offers a good convergence in all the ground-state properties. Besides, we have optimized all the geometrical structures with an energy tolerance of 1×10^{-5} eV/atom, and the forces less than 0.01 eV/Å.

Reference

1. Zhao, R. *et al.* Two-dimensional tantalum disulfide: Controlling structure and properties via synthesis. *2D Mater.* **5,** (2018).
2. Costanzo, D., Jo, S., Berger, H. & Morpurgo, A. F. Gate-induced superconductivity in atomically thin MoS 2 crystals. *Nat. Nanotechnol.* **11,** 339–344 (2016).
3. Yoshida, M. *et al.* Controlling charge-density-wave states in nano-thick crystals of 1T-TaS2. *Sci. Rep.* **4,** 1–5 (2014).
4. Cui, X. *et al.* Multi-terminal transport measurements of MoS2using a van der Waals heterostructure device platform. *Nat. Nanotechnol.* **10,** 534–540 (2015).
5. Ghorbani-Asl, M., Enyashin, A. N., Kuc, A., Seifert, G. & Heine, T. Defect-induced conductivity anisotropy in MoS 2 monolayers. *Phys. Rev. B - Condens. Matter Mater. Phys.* **88,** 1–7 (2013).
6. McDonnell, S., Addou, R., Buie, C., Wallace, R. M. & Hinkle, C. L. Defect-Dominated Doping and Contact Resistance in MoS $_2$. *ACS Nano* **8,** 2880–2888 (2014).
7. Atomistix Toolkit version 2017.2, Synopsys QuantumWise A/S. Available at: www.quantumwise.com.
8. Garrity, K. F., Bennett, J. W., Rabe, K. M. & Vanderbilt, D. Pseudopotentials for high-throughput DFT calculations. *Comput. Mater. Sci.* **81,** 446–452 (2014).
9. Schlipf, M. & Gygi, F. Optimization algorithm for the generation of ONCV pseudopotentials. *Comput. Phys. Commun.* **196,** 36–44 (2015).